Photochemistry and Photobiology, 2013, 89: 936–941

A Fiberoptic (Photodynamic Therapy Type) Device with a Photosensitizer and Singlet Oxygen Delivery Probe Tip for Ovarian Cancer Cell Killing

Dorota Bartusik[1], David Aebisher[1], Ashwini Ghogare[1], Goutam Ghosh[1], Inna Abramova[1], Tayyaba Hasan*[2] and Alexander Greer*[1]

[1]Department of Chemistry, Graduate Center, City University of New York Brooklyn College, Brooklyn, NY
[2]Wellman Center for Photomedicine, Massachusetts General Hospital and Harvard Medical School, Boston, MA

Received 12 February 2013, accepted 8 March 2013, DOI: 10.1111/php.12072

ABSTRACT

A portable "fiber optic-based sensitizer delivery" (FOSD) device has been developed and studied. Before there might be success in photodynamic therapy (PDT) and antibacterial ambitions, an understanding of basic factors on device performance was needed. Thus, the device was examined for the localized delivery of sensitizer molecules in ovarian cancer cells and production of high concentrations of singlet oxygen for their eradication *in vitro*. The device tip releases stored pheophorbide by attack of singlet oxygen from sensitized oxygen gas delivered through the hollow fiber using 669 nm laser light. The performance of the device was enhanced when configured with a fluorosilane tip by virtue of its Teflon-like property compared with a conventional glass tip (greater sensitizer quantities were photoreleased and laterally diffused, and greater amounts of ovarian OVCAR-5 cancer cells were killed). No cell damage was observed at 2.2 N of force applied by the probe tip itself, an amount used for many of the experiments described here.

INTRODUCTION

We recently reported on a sensitizer-immobilized fiber-optic device as a unique way to deactivate bacteria and photooxidize compounds in water (1,2). More recently, we developed an improved device in which photosensitization was used to release the photosensitizer from the device (3,4).

Figure 1 shows the conceptual cartoon of the "fiber optic-based sensitizer delivery" (FOSD) device and action. The device comes with a porous Vycor glass (PVG) tip that is mounted onto the terminus of the optical fiber.

Probe tip **1** is a pheophorebide photosensitizer covalently bound to PVG (Fig. 1) (3). It is a sensitizer-capped device with a photolabile di-*O*-vinyl ether bridge that releases the pheophorebide stored on the cap via attack of singlet oxygen from sensitization of the oxygen gas delivered through the hollow fiber using 669 nm laser light. *O*-Vinyl ethers are useful for photocleaving reactions at the double bond, a number of them react with $^1O_2$ by mechanisms involving dioxetane intermediates (5–8). Probe tip **1** has since been modified to probe tip **2** to improve the release action of the pheophorbide sensitizer (9).

*Corresponding author email: thasan@mgh.harvard.edu (Tayyaba Hasan); agreer@brooklyn.cuny.edu (Alexander Greer)

Probe tip **2** is a "second-generation" photosensitizer system (Fig. 1) (9). In addition to the photocleavable sensitizer, it contains a surface bound nonafluorosilane. The result is decreased absorptive affinity of the sensitizer on the probe tip surface. However, advantages of probe tip **2** over **1** go beyond the self-cleaning properties, the high number of surface fluorine atoms also produced some quenching properties that were advantageous, including reduced physical quenching of singlet oxygen by the probe interface and enhanced chemical quenching of the ethene site bonding the sensitizer to the probe tip. A formyl ester fragment remains on the surface after photodestruction of the di-*O*-vinyl ether bridge. Over time, the freed formate ester pheophorbide **3** forms the hydrolyzed benzyl ester pheophorbide **4** and parent pheophorbide-*a* **5**, a process that occurs more rapidly with base than acid (Fig. 2) (3).

We now report on our investigation into the application of the FOSD device for ovarian cancer cell eradication. Although a high number of studies have been conducted with fiber optics as light guides for hospital photodynamic therapy (PDT) applications (10), none of these fiber optics deliver sensitizer, $^3O_2$ and $^1O_2$, themselves. Development of a sensitizer and $^1O_2$ delivery device would be useful not only for cancer cell treatment but also for bacteria, in cases where local delivery might be advantageous. This study has probed into questions concerning the precise delivery of sensitizer and $^1O_2$ to ovarian cancer cells: (1) Does axial force from the probe tip damage ovarian OVCAR-5 cancer cell films, (2) can sensitizer be efficiently delivered to the cells, and is fluorine end-capped tip **2** more efficient than conventional tip **1** in doing so, and (3) what is the resultant cell viability, morphology and subcellular localization behavior?

MATERIALS AND METHODS

General information. Pyropheophorbide-*a* (**5**) was purchased from Frontier Scientific (Logan, UT). Live/Dead cell assay was purchased from Abcam Inc. (Cambridge, MA). Mitotracker Green FM fluorophore was supplied from Molecular Probes Inc. (Eugene, OR). Fetal Bovine Serum (FBS, 3D cell culture validated) was purchased from Global Cells Solution, Inc. (Charlottesville, VA). Roswell Park Memorial Institute (RPMI 1640) media and penicillin/streptomycin were purchased from Cellgrow, Mediatech Inc. (Manassas, VA). Phosphate buffered saline (PBS) was purchased from Amresco Inc. (Solon, OH). Fetal calf serum (FCS) was purchased from Invitrogen (Carlsbad, CA). Trypan Blue, DMSO, toluene-d_8 and chloroform-d_1 were purchased from Sigma-Aldrich (Allentown, PA). Microscopic glass slides (sized: 0.96 × 30 × 100 mm^3) were purchased from Corning Inc. (Corning, NY). The hemocytometer used was from Hausser Scientific (Horsham, PA). Round 29 mm glass-bottom

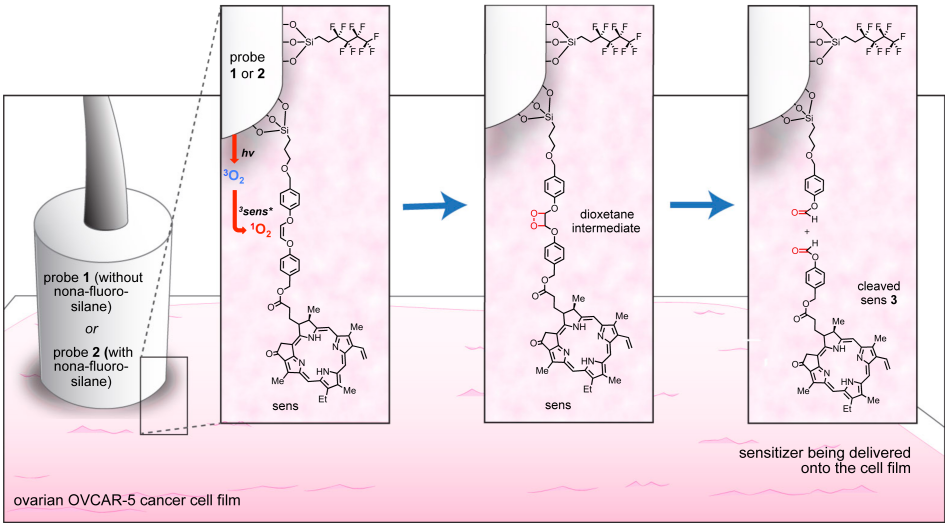

Figure 1. Cartoon of the fiber optic-based sensitizer delivery (FOSD) device action leaving behind sensitizer in cells after the alkene was converted into a dioxetane and cleaved apart. Insets: We are looking at the probe bottom, showing the sensitizer being delivered onto the cell film. The flat front face of the device tip has the sensitizer groups extended in the direction of the cell film.

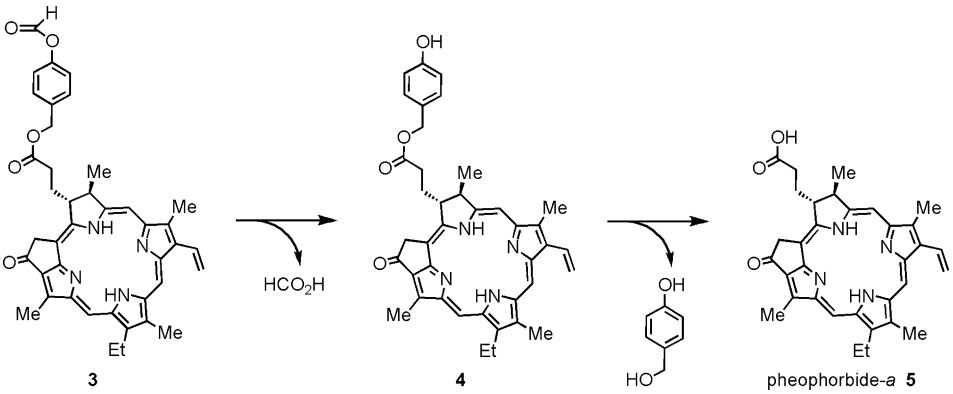

Figure 2. Pheophorbide **3** that is photocleaved from the probe tip, and the formation of hydrolysis products: Formic acid, benzyl ester pheophorbide **4**, 4-hydroxybenzylic alcohol and parent pheophorbide-*a* **5**.

dishes with 10 mm microwells dishes were purchased from In Vitro (Sunnyvale, CA). Round-bottom plates (96 wells) were purchased from Corning B. V. Life Sciences. Sterile 3 mL vials were purchased from Nalgene (Rochester, NY). Deionized water was purified using a U.S. Filter Corporation deionization system (Vineland, NJ). Porous Vycor glass was purchased from Advanced Glass and Ceramics (Holden, MA) and was dried at 500°C. A 5 mm diameter × 9 mm length bore was made into the Vycor pieces with a Dremel drill. Images of cells were obtained with a Leica confocal laser-scanning microscope (CLSM, TCS SP2, Leica, Bensheim, Germany), a Nikon TE2000 fluorescence microscope (Nikon Instruments Inc.) and an Olympus FV-1000 confocal microscope. Fluorescence images were analyzed using MetaMorph software (Molecular Devices, Downingtown, PA). Cell damage was monitored using an AmScope microscope (Irvine, CA). A Newport 1918-C power meter (Newport, Franklin, MA) and a VEGA laser power meter (Ophir Laser Measurement Group, LLC, North Logan, UT) were used for the measurement of energy of the light source. Light was delivered from a 669 nm CW diode laser (model 7404, 506 mW, 2.5 A output, Intense Inc., North Brunswick, NJ). The subcellular localization experiments used a 670 nm CW diode laser (model 7401, Intense Inc., North Brunswick, NJ).

FOSD device. A fiber-optic device with Vycor probe tips **1** and **2** was used as described previously (9). Briefly, pieces of Vycor were "fluorinated" by soaking in 1×10^{-3} M 3,3,4,4,5,5,6,6,6-nonafluorohexyltrimethoxysilane and then refluxed in toluene for 24 h. Any nonafluorosilane that was not covalently attached to the Vycor surface was washed away by Soxhlet extraction in methanol for 24 h. Prior to loading of the sensitizer and fluorosilane onto the probe tip, shaping and flattening of the tip was done with a disk grinder and polisher. The probe tips were 5 mm in diameter and 9 mm in length (~0.4 g; 165 mm^2 total area). The 5 mm diameter front face of the device tip was the operating face for these experiments. The flat shape of the bottom of the probe tip was matched to the flat shape of the OVCAR-5 films and only this front face of the cap (probe tip radius = 2.5 mm; area = 19.7 mm^2) was in contact with the cell film. The amount of sensitizer covalently bonded to the bottom plane, not the top plane or the perpendicular cylinder axis of probe tips **1** and **2** was 18 ± 1 nmol and 20 ± 1 nmol respectively (~1.2×10^{16} covalently attached sensitizer molecules). This was measured by monitoring the sensitizer Soret absorption (415 nm) after liberation from unused probe tips on dissolution with 40 (v/v)% aqueous hydrofluoric acid and extraction with dichloromethane. These tips were affixed to the hollow fiber optic with ethyl cyanoacrylate. A 3 ft long fiberoptic was used which had a Teflon gas flow inner tube running from the distal end to a T-valve. The fiber was connected to a compressed oxygen gas tank via this T-valve (operated at 4 PSI), and delivered 37 nmol O_2 through the probe tip to the ovarian cancer cells per hour. The Teflon tube was surrounded by ~60 excitation fibers randomized in a ring that was encased in a polyvinyl chloride jacket. With the fiber pinned to a translation stage, the diode laser was connected to its proximal end through an SMA connector.

Cells. OVCAR-5 ovarian carcinoma cells (Fox Chase Cancer Center, Philadelphia, PA) were grown from frozen stocks and maintained in

RPMI 1640 media, which was supplemented with 10% FCS and 1% 5000 I.U./mL penicillin/streptomycin. For the subcellular localization experiments, the RPMI media contained 10% FCS and 1% (v/v) 50 I.U./mL penicillin and 50 mg/mL streptomycin. The cells were maintained in a humidified atmosphere of 5% CO_2 at 37°C. OVCAR-5 cells were placed on a glass slide to a thickness of ~50–100 μm and a high density of cells (10^8 cells/mL) and covered an area of 625 mm^2. An area of only 19.7 mm^2 (5.3×10^5 OVCAR-5 cells) was in contact with the probe tip. The area of the front face of the probe tip to one ovarian cancer cell was ~3600:1. The extracellular space in our experiments contained a minimal amount of aqueous solution, similar to another study (11). The sensitizer that is released could reside in the extracellular space, which was ~5 (v/v)% of the film. After treatment with the device, the OVCAR-5 cell films were incubated for 20 or 30 min at 37°C, and fluorescence data were collected 1.0–1.5 h thereafter.

Dynamometer measurements. A Jamar Model 1A hand dynamometer (Sammson Preston Inc., Bolingbrook, IL) was used to measure the force delivered to the cells by the FOSD probe tip. The set-up was similar to Schmidt and Toews (12). The OVCAR-5 cells films were located on microscopic slides. Force was applied to cells by the FOSD device at increasing levels, from 0 to 44.0 N in increments of 4.4 N. Cell damage was monitored by bright-field images with the Amscope microscope at 100× magnification. The dynamometer provided a precision of 0.86 N.

Fluorescence measurements. During the 1 h reaction with the OVCAR-5 cell films, disappearance of some of the red color was observed from probe tip **2** but not **1**. An epifluorescence microscope was used with resolution of 2.0×2.7 μm and a 10× objective (excitation/emission = 560/650 nm) to quantitate sensitizer **3** that was released by the FOSD device into the OVCAR-5 cell films. Each microscope image captured a surface area measuring 3.3×3.3 mm^2. The fluorescence intensity was calculated from an average of 3 or 4 images. The fluorescence intensity was correlated with the concentration of sensitizer **3**. The fluorescence images suggested a homogeneous distribution of photoreleased **3** in the OVCAR-5 cell films, although aggregation phenomena for reduced fluorescence were not scrutinized.

Cell viability and morphology. For cell viability, experiments with the FOSD were carried out for 1 h periods with the device probe tip in contact with the OVCAR-5 cell film with the viability determined by staining with a 0.4% Trypan Blue solution (dead cells take up Trypan Blue, live cells do not). Roughly 20% of the cells treated with the FOSD device (under the center of the probe tip) were taken up with a pipette for each viability measurement. After 5 min staining with 190 μL Trypan Blue at room temperature, 30 μL of labeled cells was placed in a hemocytometer following protocols as described previously (13). Lateral distribution of 6–7 images each sized 3.3×3.3 $mm^2 = 10.9$ mm^2 was recorded each containing 5.3×10^5 cells. The time lapse between the Trypan Blue staining and microscope data collection was 10–20 min, wherein viability measurements took about 15 min to complete. For morphology, films of OVCAR-5 cells were treated with the probe tip under similar conditions as described above. The slide was scanned to find the different cellular morphologies in the FOSD device-treated sample using a total magnification of 10× and 100×. Only the 19.7 mm^2 area of the film that was treated with the FOSD device was monitored.

Sensitizer localization. The total cell population was determined as described previously (14,15). Approximately 120 000 OVCAR-5 cells were seeded in a 29 mm glass-bottom dish with a 10 mm well (In Vitro Scientific, Sunnyvale, CA) in complete RPMI media, incubated at 37°C and allowed to adhere overnight. Prior to treatment, the media were aspirated out and fresh media containing 1% (v/v) DMSO was added to the cells. After treatment with the FOSD device for 1 h, media containing 1% (v/v) DMSO was aspirated out and 2 mL fresh media was added to the cells and incubated for 24 h at 37°C. Mitotracker green (10 nmol in PBS) (excitation/emission = 490/516 nm) was added to the cells 30 minutes prior to fluorescence imaging with the Olympus confocal microscope. High-resolution images were acquired using a 40× (NA 0.45) objective lens and zoomed in 2.5 times.

RESULTS

Not too forceful

To examine whether the axial force exerted by the FOSD probe tip damaged the cells, dynamometer (strain gauge force transducer) measurements were carried out. The equivalent of finger pressure applied in pushing buttons on a computer keyboard (~9 N) (16) does not damage the cells. Forces below 31 N yielded no detectable damage to the cells. However, a force of 44.0 N led to the damage of ~20% of the cells (Fig. 3). The results in these studies were obtained over a range 4.4–44.0 N, but the majority of trials were carried out at 2.2 N.

Sensitizer cleaving "Photo Opportunity"

Table 1 and Fig. 4 show the amount of sensitizer **3** photoreleased into thin films of OVCAR-5 cells using the FOSD device equipped with Vycor probe tip **1** and **2** over 1 h. The front face of the probe tip was in contact with 5.3×10^5 OVCAR-5 cells. The amount of sensitizer **3** that cleaved free from the front face of the fluorosilane-coated fiber tip **2** (16.0 nmol) was higher than from **1** (4.6 nmol). Related to this, after photocleavage of the di-*O*-vinyl ether bridge, we found that lower amounts of sensitizer remain adsorbed onto tip **2** (1.0 nmol **3**) than tip **1** (12.4 nmol **3**).

The photoreleased sensitizer was able to diffuse to cells beyond those in direct contact with the probe tip. The net movement of sensitizer molecules was in the direction of lower concentration and did not depend much on the amount released. The sensitizer diffused laterally by 3.0 ± 0.2 mm for tip **1** and by 3.5 ± 0.5 mm for tip **2**. The cells in the *ring* around tip **2** absorbed 9.3 nmol sensitizer (Fig. 5). For the ring of cells around the probe tips, tip **2** led to greater pigmentation per cell (4.8×10^{-15} mol **3**/OVCAR-5 cell) than tip **1** (7.1×10^{-16} mol **3**/OVCAR-5 cell). Previously, the uptake of pheophorebide-*a* **5** was reported to be ~10^{-17} mol **5**/cell in SK-BR-3 and SK-OV-3 ovarian cancer cells and MDA-MB-468 breast drug-resistant cells (17). The amount of sensitizer used in these previous experiments (0.05 nmol) (17) was some 100–300 times lower to ours. As we expected, in the absence of light and flowing oxygen, the FOSD device showed no detachment of sensitizer molecules.

FOSD photodynamic treatment

As described below, we studied OVCAR-5 cell viability and morphology, and sensitizer localization after treatment with the FOSD device using probe tip **1** and/or **2**.

Cell viability and morphology. The results of sensitizer **3** release by the FOSD device into the OVCAR cell film as examined by Trypan Blue staining is shown in Fig. 6. After 1 h of exposure,

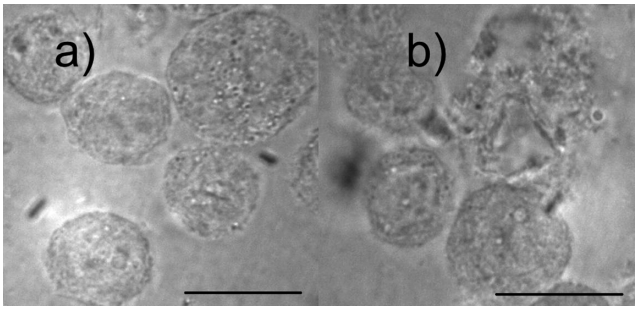

Figure 3. Force of the fiber optic-based sensitizer delivery (FOSD) probe tip onto OVCAR-5 cell film: (a) 4.4 N (no cell damage observed) and (b) 44.0 N (~20% cells damaged). Magnification 100×, bar scale = 50 μm.

Table 1. Yields of Sensitizer **3** Photoreleased and Adsorbed by Probe Tip Photooxidation into Ovarian Cancer OVCAR-5 Cell Films

entry	Vycor probe tip	Medium	photoreleased **3** (%)	photoreleased **3** (nmol)	adsorbed **3** (%)	adsorbed **3** (nmol)
1	**1**	OVCAR-5 cell film	23 ± 10	4.6 ± 2	62 ± 6	12.4 ± 1.2
2	**2**	OVCAR-5 cell film	80 ± 10	16.0 ± 2	5 ± 1	1.0 ± 0.2

[a]With Vycor probe tip **1** or **2** affixed to the hollow optical fiber, O_2 (37 nmol) and 669 nm laser light were delivered through the tip (irradiance 4.8 mW/cm^2; fluence tip = 17.28 J/cm^2, 1 h). The 37 nmol O_2 delivered to the cells is a differential and reflects a 59% increase above the 26 nmol baseline (assuming a mostly aqueous environment). The 5 mm diameter (area = 19.7 mm^2) operating front face of the device tip photodeposited sensitizer **3** into OVCAR-5 cell film (thickness: 50–100 μm; 1 mL of 10^8 cells/mL). The axial force exerted onto the samples by the probe tip was ~2.2 N. The quantity of adsorbed sensitizer was determined after the fiber optic-based sensitizer delivery (FOSD) treatment by washing the probe tips with toluene. Any excess of covalently bonded sensitizer was quantified by removal with HF and analysis of the Soret band of the sensitizer by UV-VIS spectroscopy judged against a prior constructed calibration curve of the sensitizer.

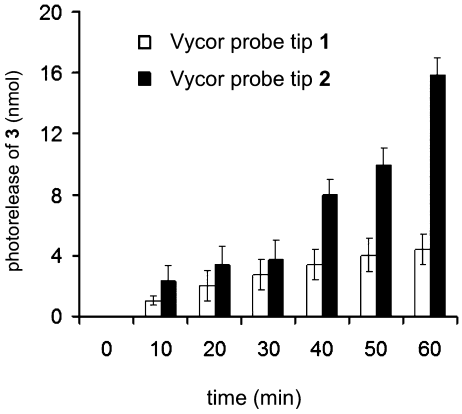

Figure 4. A time-sequence analysis of nanomols of released sensitizer **3** into OVCAR-5 cell films as a function of treatment with the fiber optic-based sensitizer delivery (FOSD) device equipped with Vycor probe tip **1** and **2**. Each value represents an average of three experiments. Axial force applied onto the cell films by the probe tip was 2.2 N.

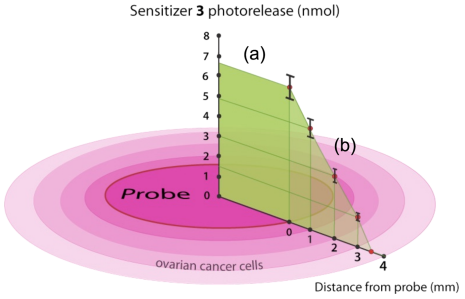

Figure 5. Sensitizer **3** released into the OVCAR-5 cell films as a function of treatment with the fiber optic-based sensitizer delivery (FOSD) device equipped with Vycor probe tip **2**. Amount of sensitizer released directly beneath the probe tip (a), and the amount that diffused away from the periphery of the probe tip (b).

the initial cell viability (95 ± 3%) was decreased by 27 ± 3% for probe tip **1** and by 60 ± 5% for probe tip **2**. Control experiments with a bare-tipped device devoid of sensitizer molecules sparging O_2 with 669 nm irradiation show viability decreases of <4%. Other control experiments showed that pheophorbide-*a* **5**, when externally added to the OVCAR-5 cell films, did not decrease cell viability in the dark, as one may expect based on similar results by others (17,18). Bright-field microscopy images of the outward appearance of OVCAR-5 cells prior to and after photooxidation with the FOSD device were compared. The cell morphology images showed noticeable photosensitized

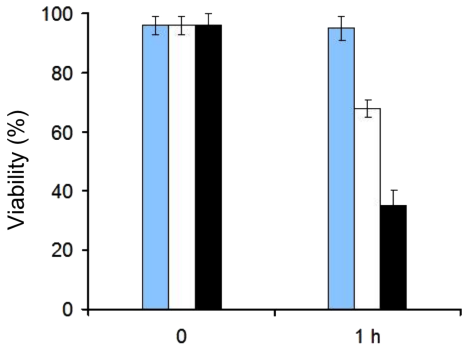

Figure 6. Comparison of viability after no exposure and after 1 hour exposure to the fiber optic-based sensitizer delivery (FOSD) device using a bare tip devoid of sensitizer molecules (blue bar), probe tip **1** (white bar) and probe tip **2** (black bar). There were 5.3 × 10^5 OVCAR-5 cells in contact with the 19.7 mm^2 face of the probe tip. The axial force applied by the probe tip was 2.2 N, and the viability was determined by Trypan Blue staining.

degradation after 1 h of exposure (data not shown), where cells were darker in color and about 30% decreased in diameter.

Localization. Subcellular localization of the sensitizer **3** photoreleased from the FOSD device equipped with probe tip **2** was also studied into a monolayer of OVCAR-5 cells (leading to pigmentation of 1.3 × 10^{-16} mol **3**/cell). Figure 7b shows the red fluorescence of sensitizer **3** (excitation/emission = 560/650 nm) that was also localized in the mitochondria based on colocalization with mitotracker green (green fluorescence, Figs. 7c and d). We also observed the localization of pheophorbide-*a* **5** in mitochondria, 24 h incubation in the absence of the photodynamic treatment. Our results are similar to previous lipophilic sensitizer results (19) and reaffirms pheophorbide localization trends (20,21). For the previously reported 2-(1-propyloxyethyl)-2-devinyl pyropheophorbide-*a*, localization was seen in the mitochondria of human pharyngeal squamous cell carcinoma (20). Pheophorbide-*a* **5** and a pheophorbide diaminobutane polypropylene-imine dendrimer complex were found to localize in the mitochondria in human leukemia (Jurkat) cells *in vitro* (21). We also saw colocalization of **3** in lysosomes, only after treatment with the FOSD device (data not shown), but did not try to distinguish between the localization effects, instead sought more fundamental insight into device performance.

DISCUSSION

Is it possible to kill cancer cells *in vitro* with the FOSD device? The FOSD device was tested, is relatively easy to use, and this

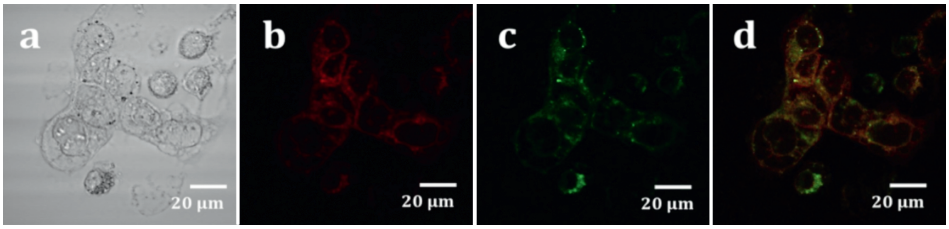

Figure 7. Subcellular localization of sensitizer **3** that was photocleaved from device tip **2** into OVCAR-5 cells after (treatment = 1 h) using fluorescence microscopy. (a) Bright-field image, (b) fluorescence image of sensitizer **3**, (c) costained with 10 nM mitotracker green and (d) overlay of images b and c. Magnification 100×.

initial study indicates that ovarian cancer cells can be killed and function well as a model system for probing questions in cancer cell treatment.

With the advent of the fluorosiliane tip **2** comes the ability to better repel the photocleaved sensitizer **3** for better device performance. The amount of sensitizer **3** cleaved free into the OVCAR cells from fluorosilane-coated fiber tip **2** was ~three-fold higher than from **1**. Our results on uptake of sensitizer by ovarian cells demonstrates that photorelease from probe tip **2** is more efficient than from tip **1**; this outcome is in agreement with results from a previous investigation (9) on photosensitizer release in toluene and in bovine tissue. These results can be understood in terms of a more efficient chemical quenching of the di-*O*-vinyl ether bridge with $^1O_2$ at the surface, and enhanced sensitizer release of the fluorosiliane tip **2** due to its Teflon-like property.

Unlike microneedles that have sharp ends for intradermal delivery of sensitizer (22), the front face of the FOSD probe tip is blunt. The front face of the probe tip was flat, averaging 5 mm in diameter, where it matched the cell film surface. The 16 nmol of sensitizer that was delivered by probe tip **2**, appears to surpass the ~0.25–2.0 nmol/mL amounts needed for PDT *in vivo* (23–25).

As indicated earlier, after the release of the formate ester sensitizer **3**, its two ester bonds can be hydrolyzed in the cells. The hydrolysis products were the benzyl ester sensitizer **4** bearing one ester bond, and free pheophorbide-*a* **5**. Ester bonds in prodrugs can persist in cells for several hours (26,27), although we are uncertain of the rate of hydrolysis of the two ester groups of **3** once delivered to the OVCAR-5 cells. The involvement of singlet oxygen and other reactive oxygen species would kill the OVCAR-5 cells by all three sensitizers **3–5** located inside and outside of the cells. The diffusion distance of $^1O_2$ itself is very limited (100–200 nm) (28,29) compared with the millimeter lateral diffusion distance of the pheophorbide sensitizer(s) in OVCAR-5 cell films.

In addition to the FOSD device above, there are devices capable of delivering singlet oxygen (30–32), including a $^1O_2$ bubbling device (33). Most, however, are configured for green chemistry and water disinfection applications rather than PDT. There remains a need for a sensitizer and $^1O_2$ delivery device to eradicate cells from complex sites with precision, such as in bacterial pockets or where interstitial PDT is carried out.

CONCLUSION

The findings with the FOSD device are encouraging. Significantly, in this study, we have probed questions into device performance for the photokilling of ovarian cancer cells, and also demonstrated that the device is suited for further development. Using the FOSD device to eradicate hypoxic cancer cells is a logical next step in the research, as well as the aim for PDT and bacterial applications to kill cells in tightly defined locations in complex 3D systems.

Acknowledgements—D.B., D.A., A.G., G.G., I.A. and A.G. acknowledge support from the NIH-National Institute of General Medical Sciences (NIH SC1GM093830). Grant support to T.H. was provided by the NIH-National Cancer Institute (5R01CA160998). We thank Mihaela Minnis for grinding and shaping of glass caps, Stanley Kimani for culturing cells and suggestions and Leda Lee for the graphic arts work. We are also thankful Zhong Wang (Hunter College Bio-Imaging Facility) and Mim Nakarmi (Brooklyn College Physics Department) for use of requisite equipment.

REFERENCES

1. Zamadar, M., D. Aebisher and A. Greer (2009) Singlet oxygen delivery through the porous cap of a hollow-core fiber optic device. *J. Phys. Chem. B* **113**(48), 15803–15806.
2. Aebisher, D., M. Zamadar, A. Mahendran, G. Ghosh, C. McEntee and A. Greer (2010) Fiber-optic singlet oxygen [$^1O_2$ ($^1\Delta_g$)] generator device serving as a point selective sterilizer. *Photochem. Photobiol.* **86**(4), 890–894.
3. Mahendran, A., Y. Kopkalli, G. Ghosh, A. Ghogare, M. Minnis, B. I. Kruft, M. Zamadar, D. Aebisher, L. Davenport and A. Greer (2011) A hand-held fiber-optic implement for the site-specific delivery of photosensitizer and singlet oxygen. *Photochem. Photobiol.* **87** (6), 1330–1337.
4. Zamadar, M., G. Ghosh, A. Mahendran, M. Minnis, B. I. Kruft, A. Ghogare, D. Aebisher and A. Greer (2011) Photosensitizer drug delivery via an optical fiber. *J. Am. Chem. Soc.* **133**(20), 7882–7891.
5. Foote, C. S. and T. R. Darling (1975) Decomposition of dioxetanes: A unique probe into mechanism and energy transfer processes". *Pure Appl. Chem.* **41**(4), 495–506.
6. Jiang, M. Y. and D. Dolphin (2008) Site-specific prodrug release using visible light. *J. Am. Chem. Soc.* **130**(13), 4236–4237.
7. Nkepang, G., P. K. Pogula, M. Bio and Y. You (2012) Synthesis and singlet oxygen reactivity of 1,2-diaryloxyethenes and selected sulfur and nitrogen analogs. *Photochem. Photobiol.* **88**(3), 753–759.
8. Klán, P., T. Solomek, C. G. Bochet, A. Blanc, R. Givens, M. Rubina, V. Popik, A. Kostikov and J. Wirz (2013) Photoremovable protecting groups in chemistry and biology: Reaction mechanisms and efficacy. *Chem. Rev.* **113**(1), 119–191.
9. Bartusik, D., D. Aebisher, G. Ghosh, M. Minnis and A. Greer (2012) Fluorine end-capped optical fibers for photosensitizer release and singlet oxygen production. *J. Org. Chem.* **77**(10), 4557–4565.
10. Fayter, D., M. Corbett, M. Heirs, D. Fox and A. Eastwood (2010) A systematic review of photodynamic therapy in the treatment of precancerous skin conditions, Barrett's oesophagus and cancers of the biliary tract, brain, head and neck, lung, oesophagus and skin. *Health Technol. Assess.* **14**(37), 1–288.
11. Chakrabarty, A., A. Mallick, B. Haldar, P. Das and N. Chattopadhyay (2007) Binding interaction of a biological photosensitizer with serum albumins: A biophysical study. *Biomacromolecules* **8**(3), 920–927.

12. Schmidt, R. T. and J. V. Toews (1970) Grip strength as measured by the Jamar dynamometer. *Arch. Phys. Med. Rehabil.* **51**(6), 321–327.
13. Freshney, R. (1987) *Culture of Animal Cells: A Manual of Basic Technique*, pp. 117. Alan R. Liss, Inc., New York.
14. Hamblin, M. R., J. L. Miller and B. Ortel (2000) Scavenger-receptor targeted photodynamic therapy. *Photochem. Photobiol.* **72**(4), 533–540.
15. Kimani, S., G. Ghosh, A. Ghogare, B. Rudshteyn, D. Bartusik, T. Hasan and A. Greer (2012) Synthesis and characterization of mono-, di-, and tri-poly(ethylene glycol) chlorin e_6 conjugates for the photokilling of human ovarian cancer cells. *J Org Chem* **77**(23), 10638–10647.
16. Berg, V. G., D. J. Clay, F. A. Fathallah and V. L. Higginbotham (1988) The Effects of Instruction on Finger Strength Measurements: Applications of the Caldwell Regime. In *Trends in Ergonomics/ Human Factors V* (Edited by F. Aghazadeh), pp. 191–198. Elsevier Science, North-Holland.
17. Savellano, M. D., B. W. Pogue, P. J. Hoopes, E. S. Vitetta and K. D. Paulsen (2005) Multiepitope HER2 targeting enhances photoimmunotherapy of HER2-overexpressing cancer cells with pyropheophorbide-*a* immunoconjugates. *Cancer. Res.* **65**(14), 6371–6379.
18. Macaroff, P. P., D. M. Oliveira, G. M. Zulmira, E. C. D. Lima, P. C. Morais and A. C. Tedesco (2005) Investigation of pheophorbide/ magnetic fluid complex as a promising system for early cancer detection and treatment. *J. Appl. Phys.* **97**(10), 10Q906.
19. Morgan, J. and A. R. Oseroff (2001) Mitochondria-based photodynamic anti-cancer therapy. *Adv. Drug Deliv. Rev.* **49**(1–2), 71–86.
20. MacDonald, I. J., J. Morgan, D. A. Bellnier, G. M. Paszkiewicz, J. E. Whitaker, D. J. Litchfield and T. J. Dougherty (1999) Subcellular localization patterns and their relationship to photodynamic activity of pyropheophorbide-*a* derivatives. *Photochem. Photobiol.* **70**(5), 789–797.
21. Paul, A., S. Hackbarth, A. Mölich, C. Luban, S. Oelckers, F. Böhm and B. Röder (2003) Comparative study of the photosensitization of Jurkat cells *in vitro* by pheophorbide-*a* and a pheophorbide-*a* diaminobutane polypropylene-imine dendrimer complex. *Laser Phys.* **3** (1), 22–29.
22. Donnelly, R. F., D. I. J. Morrow, P. A. McCarron, A. D. Woolfson, A. Morrissey, P. Juzenas, A. Juzeniene, V. Iani, H. O. McCarthy and J. Moan (2009) Microneedle arrays permit enhanced intradermal delivery of a preformed photosensitizer. *Photochem. Photobiol.* **85**(1), 195–204.
23. Laubach, H. J., S. K. Chang, S. Lee,' I. Rizvi, D. Zurakowski, S. J. Davis, C. R. Taylor and T. Hasan (2008) In-vivo singlet oxygen dosimetry of clinical 5-aminolevulinic acid photodynamic therapy. *J. Biomed. Opt.* **13**(5), 050504–1.
24. Hahn, S. M., M. E. Putt, J. Metz, D. B. Shin, E. Rickter, C. Menon, D. Smith, E. Glatstein, D. L. Fraker and T. M. Busch (2006) Photofrin uptake in the tumor and normal tissues of patients receiving intraperitoneal photodynamic therapy. *Clin. Cancer. Res.* **12**(18), 5464–5470.
25. Biel, M. (2006) Advances in photodynamic therapy for the treatment of head and neck cancers. *Lasers Surg Med* **38**(5), 349–355.
26. Lavis, L. D. (2008) Esters bonds in prodrugs. *ACS Chem. Biol.* **3**(4), 203–206.
27. Campbell, C. T., S. G. Sampathkumar and K. J. Yarema (2007) Metabolic oligosaccharide engineering: Perspectives, applications, and future directions. *Mol. BioSyst.* **3**(3), 187–194.
28. Skovsen, E., J. W. Snyder, J. D. C. Lambert and P. R. Ogilby (2005) Lifetime and diffusion of singlet oxygen in a cell. *J. Phys. Chem. B.* **109**(18), 8570–8573.
29. Redmond, R. W. and I. E. Kochevar (2006) Spatially resolved cellular responses to singlet oxygen. *Photochem. Photobiol.* **82**(5), 1178–1186.
30. Wootton, R. C. R., R. Fortt and A. J. de Mello (2002) A microfabricated nanoreactor for safe, continuous generation and use of singlet oxygen. *Org. Process. Res. Dev.* **6**(2), 187–189.
31. Lumley, E. K., C. E. Dyer, N. Pamme and R. W. Boyle (2012) Comparison of photo-oxidation reactions in batch and a new photosensitizer-immobilized microfluidic device. *Org. Lett.* **14**(22), 5724–5727.
32. Elvira, K. S., R. C. R. Wootton, N. M. Reis, M. R. Mackley and A. J. deMello (2013) Through-wall mass transport as a modality for safe generation of singlet oxygen in continuous flows. *ACS Sustain. Chem. Eng.* **1**(2), 209–213.
33. Bartusik, D., D. Aebisher, A. M. Lyons and A. Greer (2012) Bacterial inactivation by a singlet oxygen bubbler: Identifying factors controlling the toxicity of $^1O_2$ bubbles. *Environ. Sci. Technol.* **46**(21), 12098–12104.